DOI: 10.2478/sspjce-2021-0025

An attempt to apply the kinematic method of rigid solids in the study of bearing capacity of shallow foundations

Messaouda Boutahir Born Bencheikh[1,2], Assia Aidoud[1,2], Benamara Fatima Zohra[1,2], Belabed Lazhar[1,2], and Dorbani Meriem[1,2]

[1]University 8 May 1945, Laboratory of Civil Engineering and Hydraulic (LGCH), Guelma, Algeria.
[2]Faculty of science and technology, Department of civil Engineering and Hydraulics
e-mail: Bencheikh2005@yahoo.fr

Abstract

In the geotechnical engineering field, shallow foundations are frequently needed to ensure good fieldwork stability. They are also intended to permanently and uniformly transmit all load pressure on the seating floor. However, numerous mechanical constraints, such as bearing capacity of foundations, durability, stability, design of shallow foundations, lead, unfortunately, to a serious realization challenge. Finding an adequate solution presents the main goal and effort of both scholars and professionals. Indeed, the corresponding drawback is observed through the high number of reported damages that occurred in the structure of foundations and the punching failure.
The failure mechanisms of shallow foundations, verified in full size or on scale models, show "sliding surfaces" and rigid (solid) blocks, which can be described with the kinematic method of rigid solids.
The main objective of this study is the application of the kinematic method of rigid solids in the study of the stability of shallow foundations with respect to punching, the purpose of which is to determine the bearing capacity factors *Nc*, *Nγ*, and the passive earth pressure coefficient *Kp* of foundations. In this context, two mechanical models have been proposed with 5 and 7 rigid solids, and a program developed via the MathCAD environment is applied to check the validity of the two previous models. The kinematic method of rigid solids gives results very close and comparable with that of Caquot/Kerisel for the factors of the bearing capacity and passive earth pressure coefficient - the ratio *Kp* - according to the five- and seven-solid model.

Key words: bearing capacity, kinematic method of rigid solids, shallow foundations, sliding surface

1 Introduction

The problem of determining the bearing capacity of foundations, resting on a layer of soil of given resistance, constitutes one of the oldest and fundamental questions of geotechnical engineering [1]. This implies the objective of the rational sizing and designing of a footing, which safely transfers the static loads from the structure to the foundation soil.
The formulation of the load-bearing capacity problem, as well as the techniques applied for its resolution, have evolved, and continue to evolve in two directions [2,3]: (1) from a practical

point of view, following the current needs of the construction industry and the growing demand for more effective foundations and, (2) from a theoretical point of view, by enriching the known solutions, relevant for the mathematical modeling of the problem, by the adoption and the implementation of new analytical and numerical tools.
The two aspects of the problem are strongly linked, i.e., all the empirical knowledge of the construction sector and the experimental results constituted to date must be interpreted through analytical methods or reproduced through numerical models.
The problem posed is to find a new method for the evaluation of the bearing capacity of superficial foundations. Therefore, this article mainly focuses on the application of the kinematic method of rigid solids, which has been used for a long time for the stability of slopes.

In most applications of geotechnical engineering, the analysis of the stability of a slope is often a very complex issue due to the wide diversity of the sites and their heterogeneity. The kinematic method of rigid fracture solids is a very powerful tool commonly used in the limit analysis, which was described by [1]. Moreover, this method allows computing the potentialities of the system's resistance in the given geometry. This can be done by applying the principle of compatibility between the balance of this system and the resistance of its constituent material. This goal can be achieved by means of two mechanical models of possible rupture of the shallow foundations by punching, which is proposed in the following subsection, where we determine the bearing capacity factor *Nc* and passive earth pressure coefficient *Kp* of foundations. The program is developed via the MathCAD environment and applied to check the validity of the two previous models. We suppose that:

- The foundation rests on a homogeneous horizontal massif; whose behavior is characterized by cohesion and an internal friction angle.
- The effect of shear stresses at soil-foundation contact is neglected.
- No water table is present.
- The problem is modeled in two dimensions.
- The soil located above the horizontal of the base of the foundation acts as a constant vertical overload of intensity γD_f; with γ self-weight of the soil, D_f the depth or the embedding of the foundation (in this case we took $D_f = 0$).

1.1 Kinematic method of rigid fracture solids and principle of minimum safety

The type of the plastic limit state that a soil mass system reaches after sufficiently large deformations depends on the static and kinematic boundary conditions. The experience has shown that, in most cases, shallow foundations tend to break along sliding surfaces.
Therefore, the computation of the failure limit state can be carried out through the kinematic method. Compared to conventional stability checks, the rigid solid kinematic method reflects the actual mechanisms. By considering shear resistance and possible cohesion forces along secondary slip surface the system's safety reserves are properly and fully exploited [4]. It is assumed that in the state of rupture of the shallow foundations, plastic shear deformations concentrate in the slip surfaces while the rest of the soil mass does not deform (is intact). It is only under these conditions that the kinematic method of rigid failure solids can be applied [5,6].

The kinematic method of rigid break solids is based on two principles [3,7,8].

A. Principle of kinematic compatibility of potential rupture mechanisms

- Breaking mechanisms consisting of rigid solids must generally have only one degree of kinematic freedom.
- Rigid solids undergo small reciprocal movements along the slip surfaces. Solid movements are represented by a sliding plane called Hodograph.

B. Principle of minimum safety through variation in the geometry of the slip surface

All possible system-breaking mechanisms need to be studied to find the most critical mechanism with the most dangerous slip surface. Therefore, for each breaking mechanism, one must vary the inclinations of the slip surfaces as much as possible until one obtains the most critical mechanism that gives the minimum of safety [8].

The search for the mechanism of failure with minimum security, i.e., the most decisive mechanism, is systematically done in four phases [1,9]:

(1) Grouping all types of rigid solid breaking mechanisms.
(2) Formulating the boundary state equations for each mechanism.
(3) Variation of the inclinations of slip surfaces to find the geometry of the most unstable slip surfaces for each mechanism.
(4) Search for the most unstable fracture mechanism.

In the following, we will study two potential models of the rigid solid break with flat sliding surfaces. The punching of the shooting foundation in the ground is studied and subjected to a vertical load.

2 The mechanical model, including five separated rigid solids (Model I)

In this section, the study of the total equilibrium of Model I is established according to Figure 1. Accordingly, it includes five separated rigid solids, illustrated as follows. To study the total balance of Model I the five solids are separated.
The results of the Q_i (Q_{12}, Q_{23}, Q_{34}) friction forces are tilted from the angle-relative to normal on the Figure 2 slip surfaces so that their components are parallel to the slip.

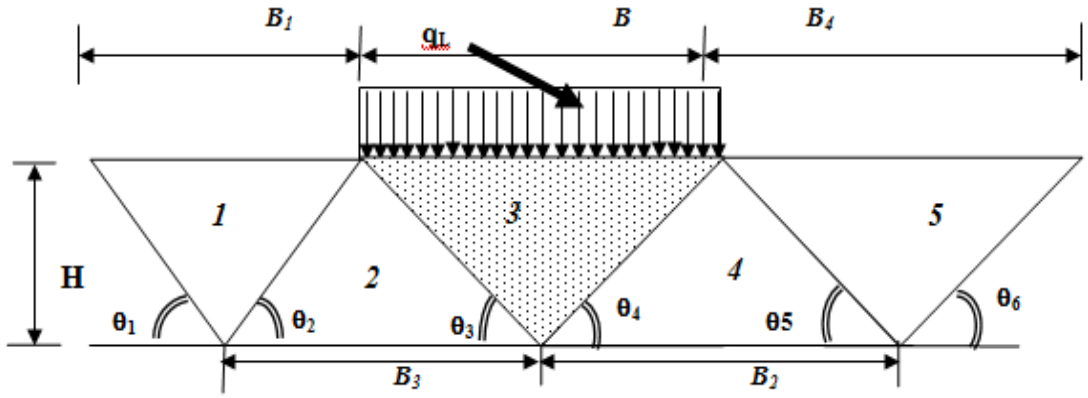


Figure 1: Failure's model including five separated rigid solids

As depicted in Figure 2, the cohesion forces *Ci* that are uniformly supplied over the sliding surfaces are computed by [3]:

$$Ci=c.li \tag{1}$$

where *Ci* the cohesion forces, *c* is the soil cohesion, *li* denotes the length of the corresponding sliding surface.

Moreover, Figure 2 shows that the previous cohesion forces also act in the opposite direction to the movement of rigid solids [10].
The position of the point of application of the forces plays no role in these models because the balance of moments is neglected [11,12,13]. The location of the friction forces Q_i on the side of the solid has no influence because we are not working with the moments.
For different types of soils and the diverse slip angles θ_1, θ_2, θ_3, θ_4, θ_5 and θ_6, the two load-bearing capacity factors $N\gamma$ and Nc can be computed for a sliding footing case. This can be done by isolating each separated body and applying the kinematic method on each one afterward. Finally, due to the complex numerical computations performed when applying the kinematic method, it is possible to reduce the number of the unknown angles $(\theta i) = 1,...,6$ using the following variable change [10,12]:

$$\theta_3 = \theta_4 = (\pi/4)+(\phi/2) \tag{2}$$

where ϕ denotes the internal friction angle.

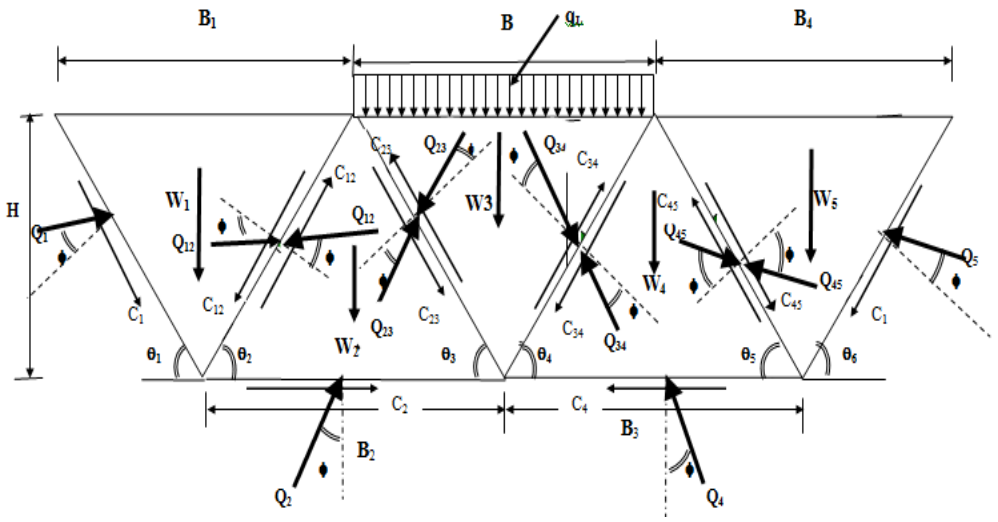


Figure 2: Presentation of deferent's strengths acting on the failure of the model with five rigid solids

To study the total equilibrium of the model (Figure 2), each solid is separated. The resultants of the friction forces Q_i are inclined by the angle ϕ with respect to the normal on the sliding surfaces so that their components parallel to the sliding surfaces act against the movement of the fracture solids. For example, the forces insulated on the solid 1 are the following: own weight w_1, Q_{12} as the force generated because of the separation of solid 2 on the solid 1 - inter-solid force, and the cohesion force C_{12}, between the two solids 1 and 2.

Therefore, the remaining angles such as θ_1, θ_2, θ_5, and θ_6 can easily be deduced according to both angles θ_3 and θ_4 [1, 12]. It yields also the two expressions (Equations A, B in the Appendix).

3 The mechanical model, including seven separated rigid solids (Model II)

The study of the total equilibrium of Model II is similarly established as the one mentioned above. Furthermore, the proposed Model II includes seven separated rigid solids (see Figure 3):

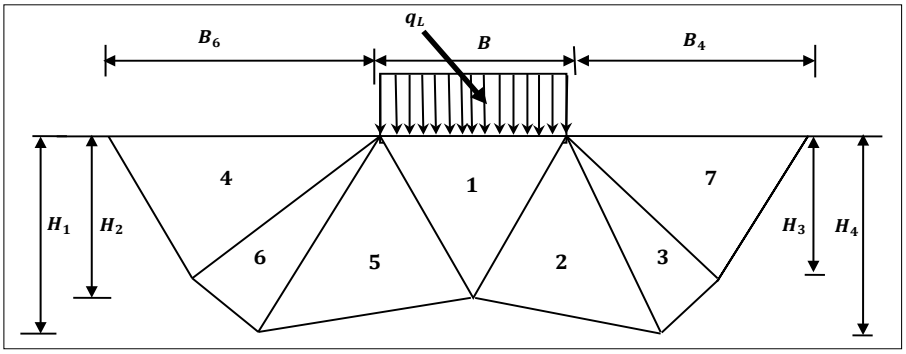


Figure 3: Failure's model including seven separated rigid solids

The same procedures are used to develop the balance equations of each solid. Finally, after the development of the equations, the general equation of the bearing capacity is obtained. The bearing capacity factors for the case of a strip footing, by applying the kinematic method of rigid fracture solids are given by Equations 3 and 4 [14]:

$$N_C = N_{C1} + N_{C2} \tag{3}$$

and

$$A = \frac{\cos(\theta_{12} - \phi)}{\sin(\theta_1 + \theta_{12} - 2\phi)},\ B = \frac{\cos(\theta_{15} - \phi)}{\sin(\theta_4 + \theta_{15} - 2\phi)} \quad and \quad C = 2\frac{\sin\theta_{15}\sin\theta_{12}}{\sin(\theta_{15} + \theta_{12})} \tag{4}$$

The Equations are further elaborated in the Appendix (C, D).

4 Parametric study

The parametric study is conducted to validate the equations found after the development of the models with five and seven rigid solids. In the next step, a program developed via the MathCAD environment is applied to check the validity of the two previous models. This test is performed only on the first model including five rigid solids, because the same results would be obtained for the seven rigid solids model. Accordingly, the given numerical results are compared with those provided by the common Caquot/Kérisel model, available in the literature. Consequently, Table 1 compares the coefficient ratios $K_{p\gamma}$ and K_{pc}, obtained with the first proposed model, and the corresponding $K_{p\gamma}$ and K_{pc}, provided by the Caquot/Kérisel model. Moreover, Table 2 compares the bearing capacity factors $N\gamma$ and Nc, given by the first proposed model, and the corresponding $N_{\gamma K}$ and N_{CK}, provided by the Caquot/Kérisel model. The comparison study is performed when the internal friction angle $\phi \in [10°, 40°]$ is gradually increased by 5° [6,14,15].

According to the calculation of bearing capacity factors *Nc* and *Ng* for the five- and seven-solid model and the model of Caquot/ Kerisel, and concerning the passive earth pressure coefficient K_p, we note a good agreement between the two models (kinematic and conventional). The kinematic model with five rigid solids gives slightly smaller limit pressures compared to the conventional model in most cases of *Ng* and *Nc*, as well as the abutment coefficients K_p limiting pressure q_L, and the bearing capacity factors.

Table 1*: Passive Earth pressure coefficient - the ratio K_p according to the five-solid model and the Caquot / Kérisel model

ϕ [°]	θ_1[°]	θ_2 [°]	θ_5 [°]	θ_6 [°]	λ [°]	$K_{P\gamma cal}$	K_{Pccal}	$K_{P\gamma K}$	K_{PcK}
10	50	50	50	50	-40	1.39	2.28	.143	1.27
15	52.5	52.5	52.5	52.5	-37.5	1.69	1.52	1.75	1.58
20	55	55	55	55	-35	2.20	1.12	2.19	1.19
25	57.5	57.5	57.5	57.5	-32.5	2.82	2.54	2.84	2.57
30	60	60	60	60	- 30	3.32	3.42	3.39	3.46
35	62.5	62.5	62.5	62.5	-27.5	5.69	4.97	5.75	5.01
40	65	65	65	65	25	9.75	8.31	9.71	8.18

The limit load q_L is calculated by applying the general equation of a strip footing subjected to a centered vertical load [16,17]:

$$q_L = \frac{1}{2}\gamma BN\gamma + cNc \tag{5}$$

(Conventional model), and by applying our general equation deduced based on the kinematic method of rigid solids (Model I kinematic) for the tilt angles of the fracture surfaces [17, 18]:

$$\theta_3 = \theta_4 = (\frac{\pi}{4} + \frac{\phi}{2}) \tag{6}$$

The results are grouped in Tables 2-5:

Table 2*: Bearing capacity factors Nc and $N\gamma$ according to the five-solid model and the model of Caquot/ Kerisel

ϕ [°]	θ_1 [°]	θ_2 [°]	θ_5 [°]	θ_6 [°]	λ [°]	$N_{\gamma cal}$	N_{ccal}	$N_{\gamma K}$	N_{cK}
10	50	50	50	50	-40	0.98	8.22	1.00	8.30
15	52.5	52.5	52.5	52.5	-37.5	2.22	10.65	2.30	11.00
20	55	55	55	55	-35	4.80	14.38	5.00	14.80
25	57.5	57.5	57.5	57.5	-32.5	9.89	20.64	10.4	20.70
30	60	60	60	60	- 30	21.64	30.68	21.8	30.10
35	62.5	62.5	62.5	62.5	-27.5	47.85	46.08	47.9	46.10
40	65	65	65	65	25	113.18	75.23	113	75.30

The values q_L in Table 3 are calculated using the Equation (7):

$$\theta_3 = \theta_4 = \frac{\pi}{4} + \frac{\phi}{2} \tag{7}$$

Table 3*: Calculated q_L values

ϕ [°] /c[kN/m²] / q_L [kN/ml]	40/0	35/5	30/10	25/20	20/35
Model I Kinematic	2037.24	1091.70	696.32	590.82	593.30
Model Conventional	2034.00	1092.70	693.40	601.20	604.40

Table 4*: Passive Earth pressure coefficient *Kp* according to the seven-solid model and the Caquot / Kérisel model

ϕ [°]	θ_1 [°]	θ_2 [°]	θ_5 [°]	θ_6 [°]	λ [°]	$K_{P\gamma cal}$	K_{Pccal}	$K_{P\gamma K}$	K_{PcK}
10	50	50	50	50	-40	1.36	2.28	.143	1.27
15	52.5	52.5	52.5	52.5	-37.5	1.59	1.52	1.75	1.58
20	55	55	55	55	-35	2.12	1.12	2.19	1.19
25	57.5	57.5	57.5	57.5	-32.5	2.72	2.54	2.84	2.57
30	60	60	60	60	- 30	3.22	3.42	3.39	3.46
35	62.5	62.5	62.5	62.5	-27.5	5.54	4.97	5.75	5.01
40	65	65	65	65	25	9.81	8.31	9.71	8.18

Table 5*: Bearing capacity factors *Nc* and $N\gamma$ according to the seven-solid model and the model of Caquot/ Kerisel

ϕ [°]	θ_1 [°]	θ_2 [°]	θ_5 [°]	θ_6 [°]	λ [°]	$N_{\gamma cal}$	N_{ccal}	$N_{\gamma K}$	N_{cK}
10	50	50	50	50	-40	1.36	2.28	.143	1.27
15	52.5	52.5	52.5	52.5	-37.5	1.59	1.52	1.75	1.58
20	55	55	55	55	-35	2.12	1.12	2.19	1.19
25	57.5	57.5	57.5	57.5	-32.5	2.72	2.54	2.84	2.57
30	60	60	60	60	- 30	3.22	3.42	3.39	3.46
35	62.5	62.5	62.5	62.5	-27.5	5.54	4.97	5.75	5.01
40	65	65	65	65	25	9.81	8.31	9.71	8.18

* The abbreviations are explained in the Appendix.

5 Conclusion

The objective of this work is to contribute to the study of the mechanical behaviour of shallow foundations with respect to punching, i.e., the study of their bearing capacity. Our contributions focused on the fundamental aspect of the problem which is the development of new mechanical models of puncture failure of shallow foundations, hence a new formulation of the bearing capacity using the kinematic approach of rigid solids. This leads to offer new tools for the treatment of relevant problems, oriented towards the new design philosophy of aesthetic, economical and reliable structures through the performance-based design.
In this paper, the stability of the shallow foundations is discussed, in which two mechanical models are proposed. The first one includes five separated rigid solids wherein the second model is characterized by seven separated rigid solids. These models allow computing the coefficient ratios as well as the bearing capacity factors for several internal friction angles. The results obtained through the five-solid model are compared with those provided by the commonly used model of Caquot/Kerisel. This comparison leads to some significant conclusions summarized as follows:

(1) Failure always occurs when the failure angle θ is greater than the internal friction angle ϕ *(*$\phi > \theta$*)*. This result is well justified physically (there is a movement of the ground).
(2) The limit load increases with increasing internal friction angle ϕ and decreasing cohesion *C*.
(3) Following the results obtained from $K_{P\gamma}$ and K_{Pc}, we note a good agreement between the two models (kinematic and conventional). The kinematic model with 5 rigid solids gives slightly smaller limit pressures compared to the conventional model in most cases N_γ and N_c, as well as the abutment coefficients $K_{P\gamma}$ limiting pressure q_L and the bearing capacity factors.
(4) The modeling accuracy of the fracture mechanisms is ensured only by the kinematic method compared to other classical methods. This allows to accurately use the resistance against shearing of the soil in the sliding surfaces as well as against the cohesion forces developed in the same areas.
(5) The choice of the kinematic method in the mechanical modeling of the stability of shallow foundations problem depends on (a) the good description of observed fracture modes and (2) it's the proper exploitation of the resistance reserves to the shear.
(6) When the inclinations of the extreme solids (dimensions) are well fixed in accordance with the active thrust theory, the corresponding inclination of the stop force is also fixed in its critical state with the same theory.
(7) The theory of the kinematic method of rigid solids reflects well the nature of ruptures of surface foundations by punching and gives realistic results.

The main drawback of the kinematic method, applied to rigid solids, is the introduction of different functions whose complexity increases with the increase in the number of rigid solids (to be considered). It depends also on the shapes of previous functions such as triangular form, curve form and so on. Further research could usefully explore the study of the stability of shallow foundations using the kinematic approach in the cases: heterogeneous soils, presence of water, or the three-dimensional analysis.

References

[1] Salençon, J 1974. *Théorie de la plasticité pour les applications à la mécanique des sols*. Eyrolles: Paris.

[2] Belabed, L 1996. *Zuverlässigkeitsuntersuchung des Tragsystems, mehrfach verankerte Stützwände"mit probabilistischen Methoden*", PhD thesis, University of Weimar, Allemagne .

[3] Belabed, L 1995. *Standsicherheitsuntersuchung zweifach verankerter Stützwände mit der kinematischen Starrkörpermethode*. *Geotechnik* 19, 171-174.

[4] Breitschaft, G. And Hanisch, J 1978. Neues Sicherheitskonzept im Bauwesen aufgrund wahrscheinlichkeitstheoretischer Überlegungen – Folgerungen fur den Grundbau unter Einbeziehung der Probenahme und der Versuchsauswertung. Vorträge der Baugrundtagung in Berlin. *Herausgegeben von der Deutschen Gesellschaft fur- und Grundbau e.v. DGEG, Essen*,659-694.

[5] Chatzigogos, C 2007. *Seismic behaviour of superficial foundations, Towards the consideration of a performance criterion in the design*. PhD thesis, Solid Mechanics Laboratory. École Polytechnique, Paris.

[6] Benamara, F.Z 2005. *Stability of walls in nail floors*. Magister's memoir, Department of Civil Engineering and Hadraulic, University of Guelma, Algérie.

[7] Zhou, X. Gu, X. Yu, M. et al 2016. Seismic bearing capacity of shallow foundations resting on rock masses subjected to seismic loads. *KSCE J Civ Engineering Geology* 20,216–228 https://doi.org/10.1007/s12205-015-0283-6.

[8] Belabed, L 1999. Application of the probabilistic safety concept on the verification of the overall stability of anchored retaining walls with the kinematics of rigid solids, *French Journal of Geotechnics* 89, 49-54.

[9] Belabed, L. and Bencheikh, M 2008. Analyse semi-probabiliste de la capacité portante des fondations superficielles. *Revue Française de Géotechnique* 124 (3), 61-75.

[10] Belabed, L 1995. *Standsicherheitsuntersuchung zweifach verankerter Stützwände mit der kinematischen Starrkörpermethode*. *Geotechnik* 19, 171-174.

[11] Zhou, XP And Cheng, H 2014. Stability analysis of three-dimensional seismic landslides using the rigorous limit equilibrium method. *Engineering Geology* 174,87-102. https://doi.org/10.1016/j.enggeo.2014.03.009.

[12] Meyerhof, G.G 1963. some recent research on the bearing capacity of foundations. *Canadian Geotechnical Journal* 1, 16-26.

[13] Salençon, J 1983. *Calculation at Break and Limit Analysis*, Paris, ENPC Press.

[14] Bencheikh, M 2010. *Analyse de la stabilité des fondations superficielles avec les méthodes probabilistes*. PhD thesis, Department of Civil Engineering and Hadraulic, University of Guelma, Algérie.

[15] Bencheikh, M 2005. *Probabilistic analysis of the stability of shallow foundations*. Magister's memoir, Department of Civil Engineering and Hadraulic, University of Guelma, Algérie.

[16] Meyerhof, G.G 1953. The bearing capacity of foundations under eccentric and inclined loads. Proceedings, *3rd International Conference on Soil Mechanics and Foundation Engineering* 3, 193 Paris.

[17] Costet, J. Sanglerat, G 1969. *Practical Course in Soil Mechanics*, Volume 2, Dunod Edition. Paris.

[18] Fakhim,i A. Villegas, T 2007. Application of dimensional analysis in calibration of a discrete element model for rock deformation and fracture. *Rock Mech Rock Eng 40:193–211*.

https:// doi.org/10.1007/s00603-006-0095-6.

Appendix

*Abbreviations used in the Tables

$N\gamma$ calculated: $N\gamma cal$,

N_c calculated: N_{ccal},

K_{Pc} calculated: KPccal,

$KP\gamma$ calculated: $K_{P\gamma\,\mathrm{cal}}$,

N_γ from coulomb and Caquot/Kerisel: $N_{\gamma K}$,

N_c from coulomb and Caquot/Kerisel: N_{cK},

$K_{P\gamma}$ from coulomb and Caquot/Keérisel: $K_{P\gamma K}$,

K_{Pc} from coulomb and Caquot/Kerisel: K_{PcK},

For our case $\beta n = 0$ (horizontal ground surface),

$\delta p = -\phi$ (since it is about the friction of the earth on itself, i.e., in the case of a stop, the passive force of the stop is inclined by the angle $\delta_p = -\phi$ (ϕ is the internal friction angle of the soil)

Equations

(A)

$$N_C = \frac{\sin\theta_4\left[\begin{array}{c}2\cos\varphi\cos\varphi\theta_1\sin(\theta_2+\theta_3)\sin(\theta_1+\theta_2-2\varphi)+\\ +\sin\theta_2\sin\theta_3\ [\cos(2\theta_1-\varphi)\sin\ (\theta_1-2\varphi)-\sin\theta_1\cos(\theta_2-\theta_1+\varphi)]\end{array}\right]}{\sin(\theta_3+\theta_4)\sin(\theta_1+\theta_2-2\varphi)\sin(\theta_3-2\varphi)\sin\theta_1\sin\theta_2} +$$

$$\frac{\sin\theta_3\left[\begin{array}{c}2\cos\varphi\cos\varphi\theta_6\sin(\theta_4+\theta_5)\sin(\theta_5+\theta_6-2\varphi)+\\ +\sin\theta_2\sin\theta_3\ [\cos(2\theta_1-\varphi)\sin\ (\theta_1-2\varphi)-\sin\theta_6\cos(\theta_5-\theta_6+\varphi)]\end{array}\right]}{\sin(\theta_3+\theta_4)\sin(\theta_5+\theta_6-2\varphi)\sin(\theta_4-2\varphi)\sin\theta_6\sin\theta_5} + 2\frac{\sin\theta_3\sin\theta_45}{\sin(\theta_3+\theta_4)}$$

(B)

$$N_\gamma = -\frac{\sin(\theta_1+\theta_2)\sin^2\theta_3\sin^2\theta_4\sin(\theta_1-\varphi)\cos(\theta_2-\varphi)\sin\theta_1\cos(\theta_2-2\varphi)}{\sin\theta_2\sin\theta_1\sin(\theta_3-2\varphi)\sin(\theta_1+\theta_2-2\varphi)\sin^2(\theta_3+\theta_4)} - \frac{\sin\theta_3\sin\theta_4}{\sin(\theta_3+\theta_4)}$$

$$+\frac{\sin(\theta_1+\theta_2)\cos(\theta_3-\varphi)\sin\varphi\sin^2\theta_4\sin\theta_3}{\sin\theta_2\sin(\theta_3-2\varphi)\sin^2(\theta_3+\theta_4)} + \frac{\sin(\theta_4+\theta_5)\cos(\theta_4-\varphi)\sin\varphi\sin^2\theta_3\sin\varphi}{\sin\theta_5\sin(\theta_4-2\varphi)\sin^2(\theta_3+\theta_4)}\times\sin\varphi$$

$$-\frac{\sin(\theta_5+\theta_6)\cos(\theta_4-\varphi)\sin(\theta_6-\varphi)\sin^2\theta_3\sin^2\theta_4\sin(\theta_5-2\varphi)\cos(\theta_4-\varphi)}{\sin\theta_5\sin\theta_6\sin(\theta_4-2\varphi)\sin(\theta_5+\theta_6-2\varphi)\sin^2(\theta_3+\theta_4)}$$

where: $N\gamma$ and Nc are the bearing capacity factors, θ_1, θ_2, θ_3, θ_4, θ_5 and θ_6 are the slip angles, and ϕ is the internal friction angle.

(C)

$$N_C = \left[A \left(\begin{array}{l} -\dfrac{\sin(\theta_{23}+\theta_{12})\sin\theta_{12}}{\sin(\theta_{15}+\theta_{12})\sin(\theta_{23}-\theta_1)}\cos(2\theta_1-\phi) \\ +\dfrac{\sin\theta_{15}\sin\theta_{12}}{\sin(\theta_{15}+\theta_{12})\sin\theta_{34}} \left(\begin{array}{l} \dfrac{\cos(\theta_{34}-\theta_2+\phi)\sin(\theta_1+\theta_{23}-2\phi)}{\sin(\theta_{23}-\theta_2)} + \\ -\dfrac{\cos(\theta_{34}-\theta_3+\phi)\sin(\theta_{34}+\theta_2-2\phi)}{\sin(\theta_{34}+\theta_3-2\phi)\sin(\theta_{23}-\theta_2)} \times \\ \sin(\theta_1+\theta_{23}-2\phi) \end{array} \right) + \\ +\dfrac{\sin\theta_1\sin\theta_{15}\sin(\theta_{23}+\theta_{12})}{\sin(\theta_{15}+\theta_{12})\sin\theta_2}\dfrac{\cos(2\theta_2-\phi)}{\sin(\theta_{23}-\theta_2)}-\dfrac{\sin\theta_{15}}{\sin(\theta_{15}+\theta_{12})}\sin(\theta_{12}-\theta_1+\phi) \\ -\dfrac{\sin\theta_1\sin\theta_{15}}{\sin\theta_3}\dfrac{\sin(\theta_1-\theta_{23})\cos(2\theta_3-\phi)\sin(\theta_{34}+\theta_2-2\phi)}{\sin(\theta_{15}+\theta_{12})\sin(\theta_{34}+\theta_3-2\phi)\sin(\theta_{23}-\theta_2)} \\ -\dfrac{\sin\theta_{12}\sin\theta_{15}\sin(\theta_1+\theta_{12})}{\sin(\theta_{15}+\theta_{12})\sin(\theta_{23}-\theta_1)} \left[\begin{array}{l} \dfrac{\sin(\theta_{23}-\theta_1)\cos(\theta_{23}+\theta_2-\phi)}{\sin(\theta_{23}-\theta_2)}+ \\ +\cos(\theta_{23}-\theta_1+\phi) \end{array} \right] \end{array} \right) \right.$$

$$\left. + B \left(\begin{array}{l} -\dfrac{\sin(\theta_{65}+\theta_{15})}{\sin(\theta_{65}-\theta_4)}\dfrac{\sin\theta_{12}}{\sin(\theta_{15}+\theta_{12})}\cos(2\theta_4-\phi) \\ +\dfrac{\sin\theta_{12}\sin\theta_{15}}{\sin\theta_{67}\sin(\theta_{15}+\theta_{12})} \left(\begin{array}{l} \dfrac{\cos(\theta_{67}-\theta_5+\phi)\sin(\theta_4+\theta_{56}-2\phi)}{\sin(\theta_{56}-\theta_5)} + \\ -\dfrac{\cos(\theta_{67}-\theta_6+\phi)\sin(\theta_{67}+\theta_5-2\phi)}{\sin(\theta_{67}+\theta_6-2\phi)\sin(\theta_{56}-\theta_5)} \times \\ \sin(\theta_4+\theta_{56}-2\phi) \end{array} \right) \\ +\dfrac{\sin\theta_{12}}{\sin(\theta_{15}+\theta_{12})}\dfrac{\sin\theta_4\sin(\theta_{65}+\theta_{15})}{\sin\theta_5}\dfrac{\cos(2\theta_5-\phi)}{\sin(\theta_{56}-\theta_5)}+ \\ -\dfrac{\sin\theta_{12}\sin\theta_{15}}{\sin\theta_{15}\sin(\theta_{15}+\theta_{12})}\sin(\theta_{15}-\theta_4+\phi) \\ -\dfrac{\sin\theta_{12}\sin\theta_{15}}{\sin\theta_6\sin(\theta_{15}+\theta_{12})}\dfrac{\sin(\theta_4-\theta_{56})\cos(2\theta_6-\phi)\sin(\theta_{67}+\theta_5-2\phi)}{\sin(\theta_{67}+\theta_6-2\phi)\sin(\theta_{56}-\theta_5)} \\ -\dfrac{\sin(\theta_4+\theta_{15})}{\sin(\theta_{65}-\theta_4)}\dfrac{\sin\theta_{12}}{\sin(\theta_{15}+\theta_{12})} \left[\begin{array}{l} \dfrac{\sin(\theta_{56}-\theta_4)\cos(\theta_{56}+\theta_5-\phi)}{\sin(\theta_{56}-\theta_5)}+ \\ +\cos(\theta_{56}-\theta_4+\phi) \end{array} \right] \end{array} \right) + 2\dfrac{\sin\theta_{15}\sin\theta_{12}}{\sin(\theta_{15}+\theta_{12})} \right]$$

(D)

$$N_\gamma = \left[\begin{array}{l} \left(\begin{array}{l} \frac{1}{2}\gamma B - \frac{\sin\theta_{12}\sin(\theta_{65}+\theta_4)\sin(\theta_4+\theta_{15})\sin(\theta_{65}+\theta_{15})}{\sin(\theta_{12}+\theta_{15})^2\sin^2(\theta_{65}-\theta_4)}\sin(\theta_4-\phi)+ \\ -\frac{\sin^2\theta_{12}\sin^2\theta_{15}\sin(\theta_5+\theta_{67})\sin(\theta_{65}-\theta_{67})}{\sin^2(\theta_{12}+\theta_{15})\sin\theta_{67}\sin(\theta_5+\theta_{65})}\frac{\sin(\theta_5-\phi)\sin(\theta_{56}-\phi)}{\sin(\theta_{56}-\theta_5)} \\ -\frac{\sin^2\theta_{12}\sin^2\theta_{15}\sin(\theta_6+\theta_{67})}{\sin^2(\theta_{12}+\theta_{15})\sin\theta_6\sin\theta_{67}}\frac{\sin(\theta_{67}+\theta_5-2\phi)\sin(\theta_6-\phi)\sin(\theta_{56}-\theta_4)}{\sin(\theta_{67}+\theta_6-2\phi)\sin(\theta_{56}-\theta_5)} \end{array} \right) \frac{\cos(\theta_{15}-\phi)}{\sin(\theta_4+\theta_{15}-2\phi)} \\ \left(\begin{array}{l} -\frac{\sin^2\theta_{15}\sin(\theta_{23}+\theta_1)\sin(\theta_1+\theta_{12})\sin(\theta_{23}+\theta_{12})}{\sin^2(\theta_{12}+\theta_{15})\sin^2(\theta_{23}-\theta_1)}\sin(\theta_1-\phi)+ \\ -\frac{\sin^2\theta_{12}\sin^2\theta_{15}\sin(\theta_2+\theta_{34})\sin(\theta_{23}-\theta_{34})}{\sin^2(\theta_{12}+\theta_{15})\sin\theta_{34}\sin(\theta_2+\theta_{23})\sin(\theta_1+\theta_{12}-2\phi)}\frac{\sin(\theta_2-\phi)\sin(\theta_{23}-\phi)}{\sin(\theta_{23}-\theta_2)} \\ -\frac{\sin^2\theta_{12}\sin^2\theta_{15}\sin(\theta_{34}+\theta_3)}{\sin^2(\theta_{12}+\theta_{15})\sin\theta_{34}\sin\theta_3}\frac{\sin(\theta_{34}+\theta_2-2\phi)\sin(\theta_3-\phi)\sin(\theta_{23}-\theta_1)}{\sin(\theta_{34}+\theta_3-2\phi)\sin(\theta_{23}-\theta_2)} \end{array} \right) \frac{\cos(\theta_{12}-\phi)}{\sin(\theta_1+\theta_{12}-2\phi)} \\ -\frac{\sin\theta_{12}\sin\theta_{15}}{\sin(\theta_{12}+\theta_{15})} \end{array} \right]$$

where: $N\gamma$ and Nc are the bearing capacity factors, θ_1, θ_2, θ_3, θ_4, θ_5 and θ_6 are the slip angles, and ϕ is the internal friction angle.